Analytical Solution for the Design of Spoolable Composite Tubing

J. Michael Starbuck[1] and Cliff Eberle[2]

REFERENCE: J. Michael Starbuck and Cliff Eberle, "Analytical Solution for the Design of Spoolable Composite Tubing," Third International Conference on Composite Materials for Offshore Operations. Houston, TX, October 31-November 2, 2000.

ABSTRACT

In oilfield spoolable tubing applications, polymer composite materials offer advantages over traditional tubing materials in terms of reduced weight and improved fatigue life. The many different loading scenarios that spoolable tubing is designed to withstand include bending strain, axial force, internal and external pressure, elevated temperature, and combinations of these loads. For the most part, these loads can be treated as axisymmetric with the exception of the bending strains. The bending strains are induced when wrapping the tubing around a large diameter spool, hence the terminology spoolable tubing. Design trade-offs occur because of the multitude of load cases and resulting multi-axial stress states promoting the need for efficient and accurate design tools. Solutions based on classical laminated shell theory are accurate for thin-wall cylinders but solutions for the three-dimensional stresses in thick-wall cylinders are needed for the typical tube diameters and wall thicknesses being considered for spoolable tubing. A closed-form solution is presented for determining the layer-by-layer stresses, strains, displacements, and first-ply failure in thick laminated composite cylinders subjected to axisymmetric and non-axisymmetric loads. The formulation is based on the theory of anisotropic elasticity and a state of generalized plane deformation along the axis of the cylinder. Parametric design trade studies can be easily and quickly computed using this closed-form solution, and a computer program that was developed for performing the numerical calculations is described.

INTRODUCTION

Spoolable tubing, better known as coiled tubing, is a well-established, intensively utilized technology in the oil industry for downhole and piping applications. Currently most coiled tubing is constructed from high strength steel. Coiled tubing services are generally perceived to be safe and reliable based on a long history of successful deployment. Nevertheless coiled steel tubing suffers from a number of performance limitations, notably low cycle fatigue,

[1] Oak Ridge National Laboratory
[2] BWXT, Y-12 Plant

"ballooning", corrosion, and limited working depth in highly deviated or horizontal boreholes [1].

Composite coiled tubing (CCT), or spoolable composite tubing, offers the potential to exceed the performance of coiled steel tubing in many cases, particularly with respect to the aforementioned performance limitations. The myriad advantages, development history, applications, and limitations of spoolable composite tubing are extensively documented [2].

Spoolable tubing must withstand many different loading scenarios, including bending strain, axial force, internal and external pressure, elevated temperature, and combinations thereof. Bending strains excepted, these loads can usually be treated as axisymmetric. The bending strains are induced by spooling and unspooling the tubing around a large diameter spool. Design trade-offs occur because of the multitude of load cases and resulting multi-axial stress states promoting the need for efficient and accurate design tools. Finite element models that are faithful to the various geometries and loading scenarios become extremely complex for non-isotropic, fiber-reinforced polymer composites. Hence analytical models based on closed-form solutions are desirable for trending and optimization studies. Such models, to be useful in spoolable composite tubing applications, must accurately resolve non-axisymmetric bending strains.

In the design and analysis of laminated composite cylinders, axisymmetric loads and axisymmetric geometries are often assumed for developing closed-form analytic solutions. In addition, the cylinder is assumed to have an infinite length such that the stresses are not only independent of the circumferential coordinate but also independent of the axial coordinate. Solutions have been formulated based on both the theory of anisotropic elasticity [3,4] and the laminated shell theory [5,6]. The laminated shell theory provides an accurate solution for thin-walled cylinders, whereas elasticity solutions are required for an accurate determination of the three-dimensional stress states that exist in thick-walled cylinders. In both of these analytical approaches, further simplifications are obtained by restricting the composite cylinder to be orthotropic.

There are a limited number of closed-form solutions for the case of axisymmetric cylinder geometries with non-axisymmetric loads. Kollar and Springer [7] considered a laminated cylinder, or cylindrical segment, subjected to hygrothermal and mechanical loads that varied in the radial and circumferential, but not in the axial direction. The theory of elasticity was used to derive the solution for stresses, strains, and displacements in the cylinder without any restrictions on ply angle and lamination sequence. The length of the cylinder was assumed to be large compared to the wall thickness and inner and outer radii such that end effects could be neglected. The only restriction on the applied mechanical loads was that they had to be in equilibrium. Pagano [8] presented a general solution for a cylindrically anisotropic cylinder subjected to surface tractions that could be expressed by a Fourier series. The surface tractions had to be independent of the axial coordinate and consistent with overall equilibrium of the cylinder. On the end faces of the cylinder, the surface tractions were prescribed as statically equivalent force and moment resultants.

ANALYTICAL FORMULATION

Single Layer Solution

The work of Pagano [8], as suggested by the author, was developed in a form that could be extended to analyze a laminated composite cylinder having anisotropic layers. This single layer solution is the foundation for the current work and the underlying assumptions and basic equations are briefly described in this section. A circular cylinder having an inner radius, r_1, and an outer radius, r_2, is considered where the stress field is independent of the axial coordinate. Traction boundary conditions are applied on the surfaces $r = r_1, r_2$, and on the end planes, independent of the axial coordinate, x, and expressed in the form of a Fourier series. The constitutive equations for a material having a single plane of symmetry ($x\theta$) with respect to a cylindrical coordinate system (x, θ, r) are written as:

$$\begin{Bmatrix} \sigma_x \\ \sigma_\theta \\ \sigma_r \\ \tau_{\theta r} \\ \tau_{xr} \\ \tau_{x\theta} \end{Bmatrix} = \begin{bmatrix} C_{11} & C_{12} & C_{13} & 0 & 0 & C_{16} \\ C_{12} & C_{22} & C_{23} & 0 & 0 & C_{26} \\ C_{13} & C_{23} & C_{33} & 0 & 0 & C_{36} \\ 0 & 0 & 0 & C_{44} & C_{45} & 0 \\ 0 & 0 & 0 & C_{45} & C_{55} & 0 \\ C_{16} & C_{26} & C_{36} & 0 & 0 & C_{66} \end{bmatrix} \begin{Bmatrix} \varepsilon_x - \alpha_x \Delta T \\ \varepsilon_\theta - \alpha_\theta \Delta T \\ \varepsilon_r - \alpha_r \Delta T \\ \gamma_{\theta r} \\ \gamma_{xr} \\ \gamma_{x\theta} - \alpha_{x\theta} \Delta T \end{Bmatrix} \tag{1}$$

The equilibrium equations in cylindrical coordinates are written as:

$$\begin{aligned} \sigma_{r,r} + \frac{1}{r}\left(\tau_{\theta r,r} + \sigma_r - \sigma_\theta\right) + F_r &= 0 \\ \tau_{xr,r} + \frac{1}{r}\left(\tau_{x\theta,\theta} + \tau_{xr}\right) &= 0 \\ \tau_{\theta r,r} + \frac{1}{r}\left(\sigma_{\theta,\theta} + 2\tau_{\theta r}\right) &= 0 \end{aligned} \tag{2}$$

where the components of stress are functions of the θ and r coordinates and the comma denotes differentiation. The F_r body force term is included and for rotational velocity is written as $\rho\omega^2 r$. The components of displacement are u, v, and w in the radial, circumferential, and axial directions, respectively, and are functions of r, θ, and x. The strain-displacement relationships are written as:

$$
\begin{aligned}
\varepsilon_r &= u_{,r} \\
\varepsilon_\theta &= \frac{1}{r}\left(u + v_{,\theta}\right) \\
\varepsilon_x &= w_{,x} \\
\gamma_{\theta r} &= v_{,r} + \frac{1}{r}\left(u_{,\theta} - v\right) \\
\gamma_{xr} &= w_{,r} + u_{,x} \\
\gamma_{x\theta} &= v_{,x} + \frac{1}{r} w_{,\theta}
\end{aligned}
\tag{3}
$$

Now by eliminating the stresses and strains from Eqn. (1)-(3) a general solution for the displacements that satisfies the compatibility equations can be written as:

$$
\begin{aligned}
u &= U(r,\theta) + \frac{x^2}{2}\left(b_1 \cos\theta - b_2 \sin\theta\right) + x\left(b_5 \cos\theta - b_6 \sin\theta\right) \\
v &= V(r,\theta) - \frac{x^2}{2}\left(b_1 \sin\theta + b_2 \cos\theta\right) - x\left(b_5 \sin\theta + b_6 \cos\theta\right) + b_3 rx \\
w &= W(r,\theta) - rx\left(b_1 \cos\theta - b_2 \sin\theta\right) + b_4 x
\end{aligned}
\tag{4}
$$

where b_i are arbitrary constants that depend on the boundary conditions. The governing equations for U, V, and W are found by substituting Eqns. (1), (3), and (4) into Eqn. (2).

$$
\begin{aligned}
&C_{33}\left(U_{,rr} + \frac{1}{r}U_{,r}\right) + \frac{C_{44}}{r^2}U_{,\theta\theta} - \frac{C_{22}}{r^2}U + \left(\frac{C_{23} + C_{44}}{r}\right)V_{,\theta r} - \left(\frac{C_{22} + C_{44}}{r^2}\right)V_{,\theta} \\
&+ \left(\frac{C_{36} + C_{45}}{r}\right)W_{,\theta r} - \frac{C_{26}}{r^2}W_{,\theta} = P_1(r,\theta) + T_1(r) \\
&\left(\frac{C_{45} + C_{36}}{r}\right)U_{,\theta r} + \frac{C_{26}}{r^2}U_{,\theta} + C_{45}V_{,rr} + \frac{C_{26}}{r^2}V_{,\theta\theta} + C_{55}\left(W_{,rr} + \frac{W_{,r}}{r}\right) + \frac{C_{66}}{r^2}W_{,\theta\theta} = P_2(r,\theta) \\
&\left(\frac{C_{23} + C_{44}}{r}\right)U_{,r\theta} + \left(\frac{C_{22} + C_{44}}{r^2}\right)U_{,\theta} + C_{44}\left(V_{,rr} + \frac{V_{,r}}{r} - \frac{V}{r^2}\right) + \frac{C_{22}}{r^2}V_{,\theta\theta} \\
&+ C_{45}\left(W_{,rr} + \frac{2}{r}W_{,r}\right) + \frac{C_{26}}{r^2}W_{,\theta\theta} = P_3(r,\theta)
\end{aligned}
\tag{5}
$$

where

$$P_1(r,\theta) = \left[(2C_{13} - C_{12})b_1 + \left(\frac{C_{45} - C_{26} + C_{36}}{r} \right) b_6 \right] \cos\theta +$$

$$\left[(C_{12} - 2C_{13})b_2 + \left(\frac{C_{45} - C_{26} + C_{36}}{r} \right) b_5 \right] \sin\theta + (C_{26} - 2C_{36})b_3 + \left(\frac{C_{12} - C_{13}}{r} \right) b_4 - \rho\omega^2 r$$

$$P_2(r,\theta) = \left[\left(\frac{C_{66} - C_{55}}{r} \right) b_5 - C_{16}b_2 \right] \cos\theta + \left[\left(\frac{C_{55} - C_{66}}{r} \right) b_6 - C_{16}b_1 \right] \sin\theta \qquad (6a)$$

$$P_3(r,\theta) = \left[\left(\frac{C_{26} - 2C_{45}}{r} \right) b_5 - C_{12}b_2 \right] \cos\theta + \left[\left(\frac{2C_{45} - C_{26}}{r} \right) b_6 - C_{12}b_1 \right] \sin\theta$$

and

$$T_1(r) = \frac{\Delta T}{r} \left[(C_{13} - C_{12})\alpha_x + (C_{23} - C_{22})\alpha_\theta + (C_{33} - C_{23})\alpha_r + (C_{36} - C_{26})\alpha_{x\theta} \right] \qquad (6b)$$

A solution to Eqn. (5) is sought subject to a set of boundary conditions that are expressed in terms of a Fourier series. Due to the rotational symmetry, the boundary conditions at the inner and outer radii are expressed in the following form:

$$\begin{aligned} \sigma_r(r_i,\theta) &= \sum_{n=0}^{\infty} p_{in} \cos n\theta \\ \tau_{\theta r}(r_i,\theta) &= q_{i0} + \sum_{n=1}^{\infty} q_{in} \sin n\theta \qquad (i = 1,2) \\ \tau_{xr}(r_i,\theta) &= t_{i0} + \sum_{n=1}^{\infty} t_{in} \sin n\theta \end{aligned} \qquad (7)$$

In Eqn. (7), the constants p_{in}, q_{in}, and t_{in} for n=0,1 are not all independent as a result of global equilibrium for the cylinder. Direct integration of the equilibrium equations results in the following relationships between the constants in Eqn. (7).

$$\begin{aligned} r_2 t_{20} &= r_1 t_{10} \\ r_2^2 q_{20} &= r_1^2 q_{10} \\ r_2 \left[\sigma_r^*(r_2) - \tau_{r\theta}^*(r_2) \right] &= r_1 \left[\sigma_r^*(r_1) - \tau_{r\theta}^*(r_1) \right] \end{aligned} \qquad (8)$$

where σ^* are the applied stress components corresponding to n = 1.

The remaining set of boundary conditions consists of the resultant axial force (F_x), torque (T), and moment (M_x) acting on any cross section of the cylinder.

$$F_x = \int_0^{2\pi}\int_{r_1}^{r_2} \sigma_x r \partial r \partial\theta$$

$$T = \int_0^{2\pi}\int_{r_1}^{r_2} \tau_{x\theta} r^2 \partial r \partial\theta \tag{9}$$

$$M_x = \int_0^{2\pi}\int_{r_1}^{r_2} \sigma_x r^2 \cos\theta \partial r \partial\theta$$

A general solution for U, V, and W is given by:

$$U(r,\theta) = \sum_{n=0}^{\infty} U_n(r)\cos n\theta + \phi_1(r,\theta)$$

$$V(r,\theta) = V_0(r) + \sum_{n=1}^{\infty} V_n(r)\sin n\theta + \phi_2(r,\theta) \tag{10}$$

$$W(r,\theta) = W_0(r) + \sum_{n=1}^{\infty} W_n(r)\sin n\theta + \phi_3(r,\theta)$$

Where $\phi_i(r,\theta)$ (i=1,2,3) correspond to the particular solution and the remaining terms are for the homogeneous solution when $P_i = T_1 = 0$. By substituting Eqn. (10) into Eqn. (5) the homogeneous solution is given by:

$$(U_n, V_n, W_n) = \sum_{s=1}^{6} (A_{ns}, B_{ns}, D_{ns}) r^{k_{ns}} \quad (n = 0,1,\mathrm{K}) \tag{11}$$

and

$$\begin{bmatrix} K_{11} & K_{12} & K_{13} \\ K_{21} & K_{22} & K_{23} \\ K_{31} & K_{32} & K_{33} \end{bmatrix} \begin{Bmatrix} A_{ns} \\ B_{ns} \\ D_{ns} \end{Bmatrix} = \begin{Bmatrix} 0 \\ 0 \\ 0 \end{Bmatrix} \tag{12}$$

$$K_{11} = \left[C_{33}k_{ns}^2 - C_{44}n^2 - C_{22}\right] \qquad K_{12} = \left[(C_{23} + C_{44})k_{ns} - C_{22} - C_{44}\right]n$$
$$K_{13} = \left[(C_{36} + C_{45})k_{ns} - C_{26}\right]n \qquad K_{21} = \left[(C_{36} + C_{45})k_{ns} + C_{26}\right]n$$
$$K_{22} = \left[C_{26}n^2 - C_{45}k_{ns}(k_{ns} - 1)\right] \qquad K_{23} = \left[C_{66}n^2 - C_{55}k_{ns}^2\right]$$
$$K_{31} = \left[(C_{23} + C_{44})k_{ns} + C_{22} + C_{44}\right]n \qquad K_{32} = \left[C_{22}n^2 - C_{44}\left(k_{ns}^2 - 1\right)\right]$$
$$K_{33} = \left[C_{26}n^2 - C_{45}k_{ns}(k_{ns} + 1)\right]$$

The determinant of the [K] matrix is set to zero and the result is a characteristic equation that is cubic in k_{ns}^2. The roots to this cubic equation provide the solution for the six constants, k_{ns}, for each value of n in the Fourier series. Special cases to the solution of Eqn. (11) occur for values of n equal to 0 and 1, where repeated roots are found for $k_{ns} = 0, 0$. For n = 0:

$$
\begin{aligned}
U_0 &= A_{03} r^{\lambda} + A_{04} r^{-\lambda} \\
V_0 &= \frac{C_{45}}{C_{44}} D_{01} + B_{05} r + \frac{B_{06}}{r} \\
W_0 &= D_{01} \ln r + D_{02} - \frac{2C_{45}}{C_{55} r} B_{06}
\end{aligned}
\tag{13a}
$$

and

$$
\lambda = \sqrt{\frac{C_{22}}{C_{33}}} \tag{13b}
$$

For the case of n = 1:

$$
\begin{aligned}
U_1 &= A_{11} + A_{12} \ln r \\
V_1 &= -A_{11} - A_{12} \left\{ \left[\frac{C_{26} C_{36} - C_{66}(C_{23} + C_{44})}{C_{26}^2 - C_{66}(C_{22} + C_{44})} \right] + \ln r \right\} \\
W_1 &= -A_{12} \left[\frac{C_{26}(C_{23} + C_{44}) - C_{36}(C_{22} + C_{44})}{C_{26}^2 - C_{66}(C_{22} + C_{44})} \right]
\end{aligned}
\tag{14}
$$

The particular solution in Eqn. (10) is found by direct substitution into Eqn. (5) and is:

$$
\begin{aligned}
\phi_1(r,\theta) &= \left(a_1 b_4 + \frac{\Delta T \beta}{C_{33} - C_{22}} \right) r + a_2 b_3 r^2 - \left(\frac{\rho \omega^2}{9C_{33} - C_{22}} \right) r^3 + a_3 r^2 (b_1 \cos\theta - b_2 \sin\theta) \\
\phi_2(r,\theta) &= a_4 r^2 (b_1 \sin\theta + b_2 \cos\theta) \\
\phi_3(r,\theta) &= a_5 r^2 (b_1 \sin\theta + b_2 \cos\theta) - r(b_5 \cos\theta + b_6 \sin\theta)
\end{aligned}
\tag{15}
$$

where

$$
\begin{aligned}
a_1 &= \frac{C_{12} - C_{13}}{C_{33} - C_{22}} \\
a_2 &= \frac{C_{26} - 2C_{36}}{4C_{33} - C_{22}} \\
\beta &= (C_{13} - C_{12})\alpha_x + (C_{23} - C_{22})\alpha_\theta + (C_{33} - C_{23})\alpha_r + (C_{36} - C_{26})\alpha_{x\theta}
\end{aligned}
\tag{16}
$$

and a_3, a_4, and a_5 are found by solving the following set of three simultaneous linear equations.

$$\begin{bmatrix} (4C_{33} - C_{44} - C_{22}) & (2C_{23} + C_{44} - C_{22}) & (2C_{36} + 2C_{45} - C_{26}) \\ (2C_{36} + 2C_{45} + C_{26}) & (C_{26} - 2C_{45}) & (C_{66} - 4C_{55}) \\ (2C_{23} + 3C_{44} + C_{22}) & (C_{22} - 3C_{44}) & (C_{26} - 6C_{45}) \end{bmatrix} \begin{Bmatrix} a_3 \\ a_4 \\ a_5 \end{Bmatrix} = \begin{Bmatrix} 2C_{13} - C_{12} \\ C_{16} \\ C_{12} \end{Bmatrix} \tag{17}$$

Finally, due to the form of the prescribed boundary conditions in Eqn. (7) $b_2 = 0$ and neglecting rigid body motions results in:

$$b_5 = b_6 = A_{11} = B_{05} = D_{02} = 0 \tag{18}$$

The solution for a single layer, as described by the above equations, is applicable for all fiber orientations with some minor changes to the equations for orthotropic ($C_{16} = C_{26} = C_{36} = C_{45} = 0$) and transversely-isotropic ($C_{12} = C_{13}$, $C_{22} = C_{33}$, $C_{55} = C_{66}$, $C_{44} = ½(C_{22} - C_{23})$ layers. Taking the highest index in the Fourier series to be M, the actual solution to the problem contains 6M + 6 unknowns and there are 6M + 6 independent equations. The unknown constants are b_1, b_3, b_4, A_{03}, A_{04}, A_{ij} (j = 2,3,…,6), B_{06}, D_{01}, and A_{ns} (s = 1,2,…,6, $2 \le n \le M$). Some of the details have been omitted for brevity here but can be found in the original work of Pagano [8].

Laminate Solution

For a laminated cylinder, the solution described in the previous section is applied to each layer and interfacial continuity is invoked between neighboring layers. The boundary conditions at the inner and outer radii of the cylinder are applied to the inner radius of the first layer and the outer radius of the last layer, respectively. Let R_1 and R_2 be the cylinder inner and outer radii, respectively, $r_1^{(k)}$ and $r_2^{(k)}$ be the inner and outer radii of the k^{th} layer, and t_k be the thickness of the k^{th} layer. For N layers there are N-1 interfaces and by using the following notation:

$$r_1^{(1)} = R_1 \qquad r_2^{(N)} = R_2 \qquad r_1^{(k)} = r_2^{(k-1)} \qquad r_k = r_2^{(k)} = r_1^{(k)} + t_k \tag{19}$$

the continuity equations for k = 1,2,…N-1 are written as:

$$\begin{aligned} \sigma_r^{(k)}\left(\theta, r_2^{(k)}\right) &= \sigma_r^{(k+1)}\left(\theta, r_1^{(k+1)}\right) \\ \tau_{\theta r}^{(k)}\left(\theta, r_2^{(k)}\right) &= \tau_{\theta r}^{(k+1)}\left(\theta, r_1^{(k+1)}\right) \\ \tau_{xr}^{(k)}\left(\theta, r_2^{(k)}\right) &= \tau_{xr}^{(k+1)}\left(\theta, r_1^{(k+1)}\right) \\ u^{(k)}\left(\theta, r_2^{(k)}\right) &= u^{(k+1)}\left(\theta, r_1^{(k+1)}\right) - \delta_k\left(\theta, r_k\right) \\ v^{(k)}\left(\theta, r_2^{(k)}\right) &= v^{(k+1)}\left(\theta, r_1^{(k+1)}\right) \\ w^{(k)}\left(\theta, r_2^{(k)}\right) &= w^{(k+1)}\left(\theta, r_1^{(k+1)}\right) \end{aligned} \tag{20}$$

where δ_k is a prescribed interference between layers. The resultant force and moment given by Eqn. (9) are modified to be a summation over all the layers and are rewritten as:

$$F_x = \sum_{k=1}^{N} \int_0^{2\pi} \int_{r_1^k}^{r_2^k} \sigma_x^k r \partial r \partial \theta$$

$$T = \sum_{k=1}^{N} \int_0^{2\pi} \int_{r_1^k}^{r_2^k} \tau_{x\theta}^k r^2 \partial r \partial \theta \qquad (21)$$

$$M_x = \sum_{k=1}^{N} \int_0^{2\pi} \int_{r_1^k}^{r_2^k} \sigma_x^k r^2 \cos\theta \partial r \partial \theta$$

Recall that each layer has 6M + 6 unknown constants and therefore, the solution to the problem of a cylinder having N layers has 6N(M + 1) unknown constants. There are 6M + 6 independent equations from the boundary conditions and 6(N – 1)(M + 1) from the continuity equations for a total of 6N(M+1) equations.

The solution procedure is divided into three separate parts that depend on the number of terms in the Fourier series. For n = 0 in the Fourier series there are 4N simultaneous equations that are used to solve for the 4N unknowns of $b_3^{(k)}$, $b_4^{(k)}$, $A_{03}^{(k)}$, and $A_{04}^{(k)}$. There are 4(N – 1) equations from continuity of radial stress and continuity of the three displacement components. The remaining 4 equations are from the radial stress boundary conditions at the inner and outer radii of the cylinder (p_{10} and p_{20}) and from the resultant axial force and torque conditions. The 2N unknowns of $D_{01}^{(k)}$ and $B_{06}^{(k)}$ are solved from continuity of the two shear stress components (2N – 2 equations) and the two boundary conditions for shear stress at the inner radius of the cylinder (q_{10} and t_{10}). For n = 1, there are 6N unknowns with 6(N – 1) equations from continuity of the three stress and three displacement components and 6 equations from the boundary conditions corresponding to the terms of p_{11}, p_{21}, q_{11}, t_{11}, and t_{21}, and the resultant moment. The unknowns are $b_1^{(k)}$, $A_{12}^{(k)}$, and $A_{1s}^{(k)}$ (s = 3,4,5,6). Finally, for each n = 2,3,,,M a 6N X 6N system of equations is solved for the 6N(M – 1) unknowns of $A_{ns}^{(k)}$ (s = 1,2,…,6). There are 6(N – 1)(M – 1) equations from the 6 continuity equations and there are 6(M – 1) equations from the boundary conditions terms of p_{1n}, p_{2n}, q_{1n}, q_{2n}, t_{1n}, and t_{2n}.

A FORTRAN program has been developed for performing the calculations described in the above solution procedure. The program is general in the sense that monoclinic, orthotropic, and transversely-isotropic layers can be analyzed, and multiple material systems are acceptable. The layer-by-layer stresses, strains, and displacements are calculated in both the global cylindrical coordinate system and in the layer principal material directions.

Failure Criteria

Failure criteria for determining first-ply failure are implemented in the program based on using Hashin's criteria [9] and the Tsai-Wu criterion [10]. These are three-dimensional failure criteria that take into account the stress interactions that occur in composite materials having multi-axial stress states. Hashin's criteria are quadratic stress polynomials expressed

in terms of the transversely isotropic invariants of the applied average stress state. Four distinct failure modes are modeled separately resulting in a piecewise smooth failure surface. The four modes are tensile fiber mode, compressive fiber mode, tensile matrix mode, and compressive matrix mode. The equations in Hashin's paper are rewritten here in terms of a safety factor, R, defined by

$$\{\sigma\}_{MAX} = R\{\sigma\}_{APPLIED} \tag{22}$$

where $\{\sigma\}_{APPLIED} = \{\sigma_{11},\sigma_{22},\sigma_{33},\tau_{12},\tau_{13},\tau_{23}\}$ is the principal material direction stress vector resulting from the applied loads and $\{\sigma\}_{MAX} = \{X_T,X_C,Y_T,Y_C,S_A,S_T\}$ is the allowable strength vector with X, Y, and S corresponding to the fiber direction, transverse direction, and shear strengths, respectively.

Tensile Fiber Mode: $\sigma_{11} > 0$

$$R = \frac{1}{\sqrt{\left(\frac{\sigma_{11}}{X_T}\right)^2 + \left(\frac{\tau_{12}}{S_A}\right)^2}} \tag{23}$$

Compressive Fiber Mode: $\sigma_{11} < 0$

$$R = -\left(\frac{X_C}{\sigma_{11}}\right) \tag{24}$$

Tensile Matrix Mode: $\sigma_{22} + \sigma_{33} > 0$

$$R = \left\{\left(\frac{\sigma_{22}+\sigma_{33}}{Y_T}\right)^2 - \left(\frac{\sigma_{22}\,\sigma_{33}}{S_T^2}\right) + \left(\frac{\tau_{12}}{S_A}\right)^2\right\}^{-1/2} \tag{25}$$

Compressive Matrix Mode: $\sigma_{22} + \sigma_{33} < 0$

$$R^2\left\{\left(\frac{\sigma_{22}+\sigma_{33}}{2S_T}\right)^2 - \left(\frac{\sigma_{22}\,\sigma_{33}}{S_T^2}\right) + \left(\frac{\tau_{12}}{S_A}\right)^2\right\} + R\left\{\left(\frac{\sigma_{22}+\sigma_{33}}{Y_C}\right)\left[\left(\frac{Y_C}{2S_T}\right)^2 - 1.0\right]\right\} = 1.0 \tag{26}$$

LOAD CASES

Consider a T300/862 graphite/epoxy angle-ply tube having an inner diameter of 1.0 inch and an outer diameter of 1.5 inches. The unidirectional orthotropic material properties used in the analyses are provided in Table 1. To demonstrate the usage of the analysis method described above, results are presented by plotting the maximum allowable load (calculated from the R safety factor) as a function of the helical angle used in the angle-ply laminate.

The maximum internal pressure corresponds to a helical angle of 80° (see Figure 1). Note that the symbols used in the plots correspond to the first-ply failure mode as predicted by the Hashin criteria. For internal pressure the mode changes from matrix to fiber at 45° and then back to a matrix mode at helical angles greater than 85°. For external pressure, the maximum pressure capability that is shown in Figure 1 corresponds to an angle of 90°, i.e., an all-hoop wound tube. The tube fails due to a tensile matrix mode (TMM) for angles greater than 45°. At angles less than 45°, compressive matrix mode (CMM) is predicted with the exception of angles between 25-35° where failure due to a tensile fiber mode (TFM) is predicted. As one would expect, the maximum axial tensile load capacity is for a 0° angle and the mode switches from fiber to matrix at an angle of 45° (see Figure 2).

Wrapping the tubing around spool diameters that are typically around 6-7 feet in diameter induces the bending strain [11] and the bending of the tubing results in a non-axisymmetric stress distribution. To analyze the spooling load scenario, an applied resultant end moment is used. For typical tube outer diameters of 1.5 in. [11] on a 6-foot spool diameter the bending strain, ε_0, is equal to 2.0%. This is calculated by dividing the distance from the neutral axis by the radius of curvature. The applied moment necessary to produce this bending strain is a function of the tube geometry and lamination sequence and can be estimated by:

$$M = \frac{\varepsilon_0}{R_2}\sum_{k=1}^{N} E_{xk} I_k = \frac{\pi\varepsilon_0}{4R_2}\sum_{k=1}^{N} \left(r_2^4 - r_1^4\right)_k E_{xk} \tag{27}$$

where E_{xk} and I_k are the k^{th} layer axial stiffness and layer moment of inertia [12]. This is a laminated beam theory approach that considers the stiffness of each individual ply. Alternatively, an averaging approach can be taken and an effective laminate axial stiffness can be calculated using the micromechanics approach of either Sun and Li [13] or Greszczuk [14]. Using this approach the moment is estimated by:

$$M = \frac{\varepsilon_0}{R_2} E_{xeff} I = \frac{\pi\varepsilon_0}{4R_2} E_{xeff}\left(R_2^4 - R_1^4\right) \tag{28}$$

Figure 3 shows that the moments calculated using Equations (27) and (28) are significantly different when the angle is not equal to zero and not greater than 70° with the effective axial stiffness method being consistently higher than the laminated beam theory method. The maximum bending strain as function of helical angle is plotted in Figure 4 using both methods for estimating the moment. The tube is predicted to have a fiber failure mode for angles less than 35° and a matrix mode for angles greater than 35°. For angles less than 5° the failure in the fiber direction is a compressive mode (CFM).

The maximum bending strain capability is shown to be at very shallow helical angles. Larger maximum bending strains are predicted when the applied moment is estimated by the beam theory approach. In either approach, the calculated axial strains in the tube are not equal to the applied bending strain used to estimate the applied moment. The only exception to this is when the fiber orientation is 0°. It is not clear to the author which method should be used or if alternative approaches need to be investigated.

CONCLUSIONS

A closed-form solution has been presented for design and analysis of an axisymmetric laminated cylinder subjected to non-axisymmetric loads. The solution is based on the theory of anisotropic elasticity and an assumed generalized plane deformation state of stress. The prescribed boundary conditions are expressed in terms of a Fourier series and are independent of the axial coordinate. Using zero terms in the Fourier series expansion treats the special case of axisymmetric loads. The solution is general in that monoclinic, orthotropic, transversely-isotropic, and isotropic layers are considered in the formulation and multiple material systems may be used. The prescribed loads include axial force, moment, torque, internal and external pressure, uniform temperature change, and rotational velocity with interference fits. A FORTRAN code was developed for performing the necessary calculations and the code can be executed from a desktop computer. This permits a computationally efficient method for conducting numerous design trade studies.

The utilization of the code for CCT applications was demonstrated by analyzing the response of a graphite/epoxy angle-ply laminate that was subjected to different CCT loads. Depending on the design specifications and loading scenarios, different angle-ply laminate architectures were shown to be required. Further validation of this solution procedure for CCT design is needed to resolve the approach taken in estimating the applied moment for simulating the spooling load case.

ACKNOWLEDGEMENTS

Oak Ridge National Laboratory is managed by UT-Battelle, LLC, for the U.S. Department of Energy under contract DE-AC05-00OR22725.

REFERENCES

1. A. Sas-Jaworsky II and J. G. Williams, “Development of Composite Coiled Tubing for Oilfield Services,” SPE paper 26536, presented at 68th Annual Technical Conference and Exhibition of the Society of Petroleum Engineers, Houston, TX, October, 1993.

2. J. G. Williams and A. Sas-Jaworsky II, “Composite Spoolable Pipe Development, Advancements, and Limitations,” Offshore Technology Conference paper 12029, Houston, TX, May, 2000.

3. M. W. Hyer, “Hydrostatic Response of Thick Laminated Composite Cylinders,” Jrl. Reinforced Plastics and Composites, Vol. 7, 1988, p321.

4. A. K. Roy and S. W. Tsai, “Design of Thick Composite Cylinders,” Jrl. of Pressure Vessel Tech., Trans. of ASME, Vol. 110, 1988, p255.

5. S. A. Ambartsumyan, “Theory of Anisotropic Shells, NASA Technical Translation, NASA TTF-118,” 1964.

6. J. M. Whitney, “On the Use of Shell Theory for Determining Stresses in Composite Cylinders,” Jrl. Comp. Matl., Vol. 5, 1971, p340.

7. L. P. Kollar and G. S. Springer, “Stress Analysis of Anisotropic Laminated Cylinders and Cylindrical Segments,” Int. J. Solids Structures, Vol. 29, No. 12, 1993, p1499.

8. N. J. Pagano, “The Stress Field in a Cylindrically Anisotropic Body Under Two-Dimensional Surface Tractions,” Jrl. Appl. Mech., 1972, p791.

9. Z. Hashin, “Failure Criteria for Unidirectional Fiber Composites,” Jrl. App. Mech., Vol. 47, 1980, p329.

10. S. W. Tsai and E. M. Wu, “A General Theory of Strength for Anisotropic Materials,” Jrl. Comp. Matl., Vol. 5, 1971, p58.

11. R. M. Sorem and S. Bona, “Comparison of FEA and Classical Plate Theory for Thick-Walled Composite Tubing,” Proc. Energy Sources Technology Conference and Exhibition, ETCE98-4604, ASME, 1998.

12. J. M. Whitney, Structural Analysis of Laminated Anisotropic Plates, Technomic Publishing Company, Lancaster, PA, 1987, p. 69.

13. C. T. Sun and Sijian Li, “Three-Dimensional Effective Elastic Constants for Thick Laminates,” Journal of Composite Materials, Vol. 22, July, 1988, pp. 629-639.

14. L. B. Greszczuk, Elastic Constants and Analysis Methods for Filament Wound Shell Structures, SM-45849, Missile and Space Systems Division, Douglas Aircraft Company, January, 1964.

Table 1. T300/862 Composite Material Properties

Property	Value
E11 (Msi)	20.21
E22 = E33 (Msi)	1.101
ν12 = ν13	0.3264
ν23	0.3642
G12 = G13 (Msi)	0.5495
G23 (Msi)	0.4035
Xt (psi)	261,000
Xc (psi)	250,000
Yt (psi)	6,000
Yc (psi)	30,000
Sa (psi)	10,000
St (psi)	3,000

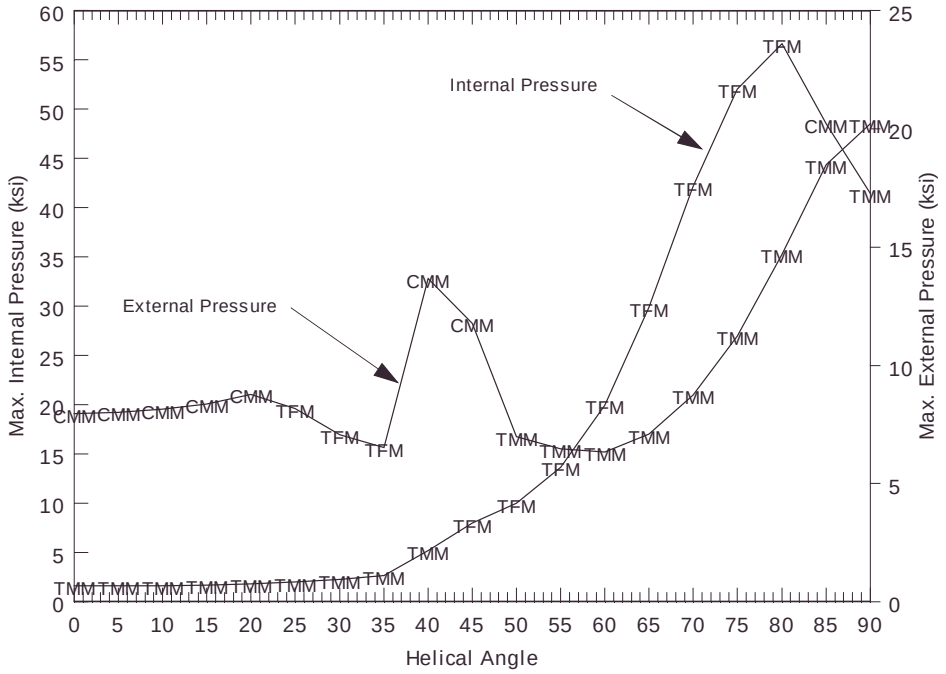

Figure 1. Maximum internal and external pressure for angle-ply graphite/epoxy tube.

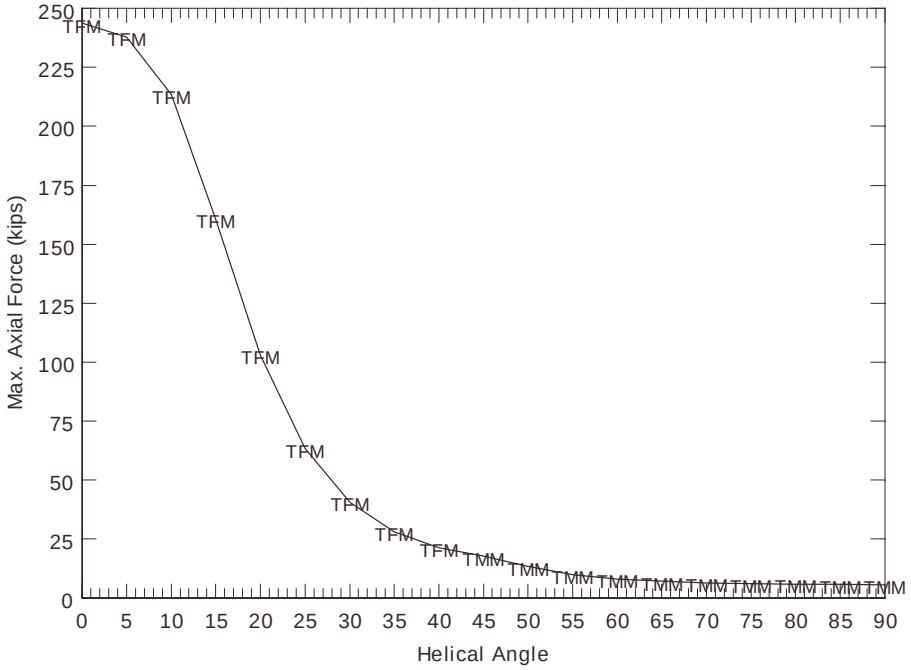

Figure 2. Maximum axial force for angle-ply graphite/epoxy tube.

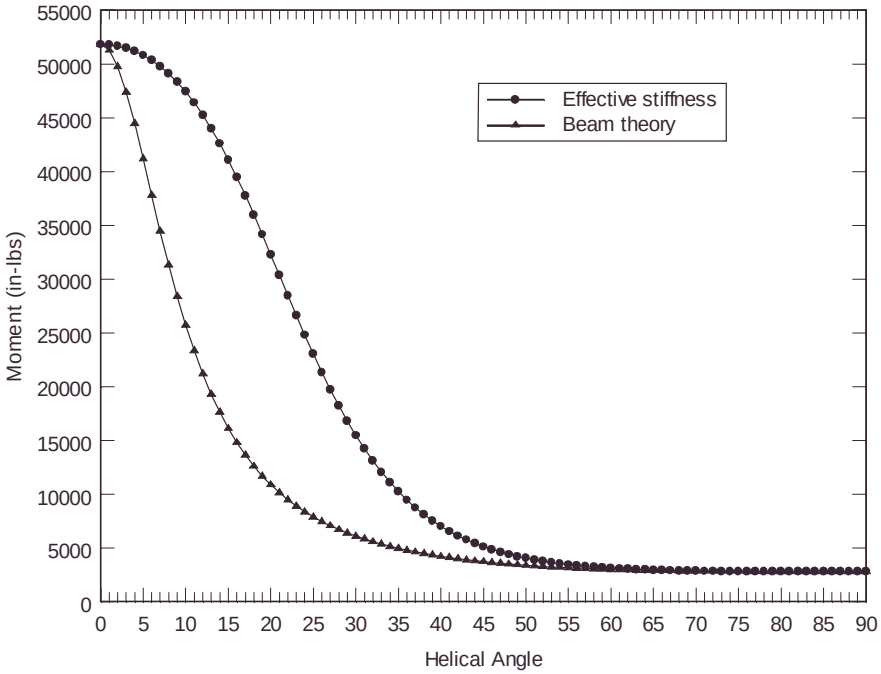

Figure 3. Estimated bending moment per unit axial strain.

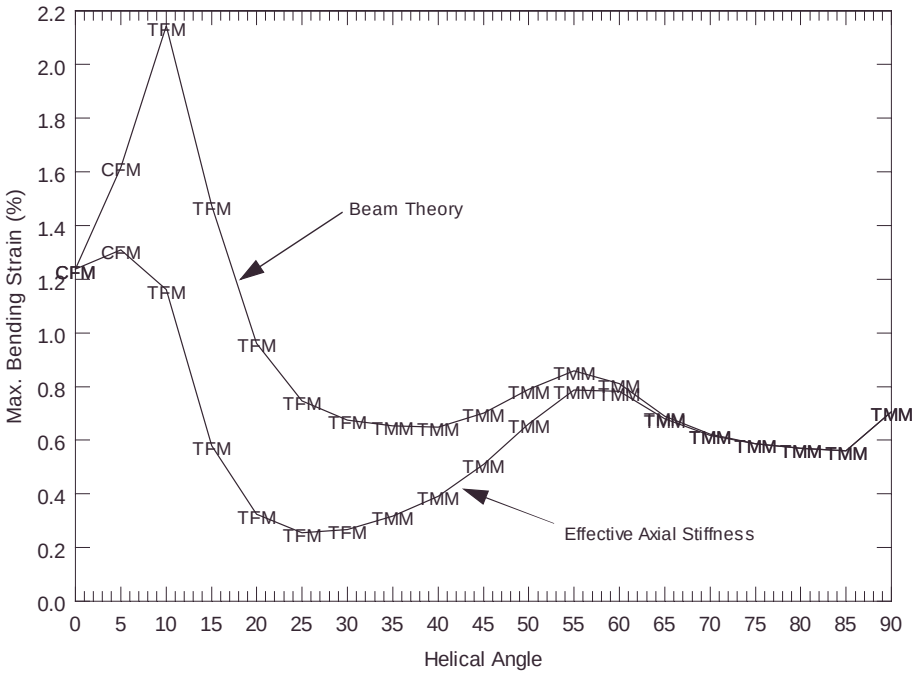

Figure 4. Maximum bending strain for angle-ply graphite/epoxy tube.